NUCLEAR SCIENCE AND TECHNIQUES **25**, 060301 (2014)

Radiation synthesis of polymer/clay nanocomposite hydrogels with high mechanical strength*

MA Rong-Fang (马荣芳),[1] YUAN Jie (袁劼),[1] LI Can-Can (李灿灿),[2] PENG Jing (彭静),[1]
DONG Zhen (董珍),[1] XU Ling (许零),[3] LI Jiu-Qiang (李久强),[1] and ZHAI Mao-Lin (翟茂林)[1,†]

[1]*Beijing National Laboratory for Molecular Sciences, Radiochemistry and Radiation Chemistry Key Laboratory of Fundamental Science, the Key Laboratory of Polymer Chemistry and Physics of the Ministry of Education, College of Chemistry and Molecular Engineering, Peking University, Beijing 100871, China*
[2]*School of Materials and Engineering, University of Science and Technology Beijing, Beijing 100083, China*
[3]*Department of Energy and Resources Engineering, College of Engineering, Peking University, Beijing 100871, China*
(Received April 29, 2014; accepted in revised form May 19, 2014; published online December 15, 2014)

Poor mechanical properties of PNIPAAm hydrogels have limited their applications. Nanocomposite hydrogels (NC gels) which incorporate inorganic clay possess high mechanical strength and other desirable properties. In this paper, we report a facile approach to synthesize NC gels using radiation technique. With exfoliated clay sheets acting as crosslinkers, *N*-isopropylacrylamide monomers are polymerized and crosslinked to form NC gels under γ-irradiation at room temperature. Apart from regular swelling behavior and interesting performance in thermo sensitivity, the radiation synthesized NC gel (RNC gel) has good optical transparency, high strength and flexibility. Through Micro-FTIR, XPS and TG analyses, a particular chemically crosslinked organic/inorganic network was identified in the RNC gel.

Keywords: Clay, Mechanical properties, Irradiation, Stimuli-sensitive polymers, Composites

DOI: 10.13538/j.1001-8042/nst.25.060301

I. INTRODUCTION

Poly(*N*-isopropylacrylamide) (PNIPAAm) hydrogels are typical thermo sensitive materials. They change their volume abruptly and significantly on temperature variations from external environments, and exhibit a lower critical solution temperature (LCST) at about 33 °C [1]. Multi-responsive hydrogels based on PNIPAAm have been developed using various methods. For instance, double sensitive hydrogels responding to pH and temperature can be obtained by combining comonomers containing particular groups with NIPAAm [2]. Photothermally sensitive hydrogels [3] and electrosensitive hydrogels [4] based on PNIPAAm were developed recently. Due to their unique properties, PNIPAAm hydrogels found their applications in chemical devices [5], tissue engineering [6], microfluidic actuators [7], separation [8], biomedical fields [9], etc.

However, application of PNIPAAm hydrogels is limited by their poor mechanical properties. Several strategies have been employed to improve the mechanical strength of PNIPAAm hydrogels, such as developing gels with topological structure [10], introducing a double network structure into PNIPAAm hydrogels [11] and synthesizing nanocomposite gels (NC gels) [12], of which NC gels have intrigued much research interests because of their desirable properties [13, 14].

Laponite is a synthetic hectorite consisting of layered magnesium silicate platelets in sizes of Φ20–30 nm×1 nm [15]. Reactive Si−OH groups and Mg−OH (or Li−OH) groups are present on the surface of laponite clay sheets [16]. Laponite clay has been introduced into a polymer matrix generated from amide monomers to form novel NC gels with outstanding mechanical strength and optical properties. Proper catalysts and initiators that have strong physical interactions with the clay sheet surface were necessary for preparing NC gels [12, 15]. A novel three-dimensional network was formed in the NC gel with clay sheets acting as multifunctional crosslinkers. This physically crosslinked network showed wonderful self-healing function due to the reversibility of physical interactions [17].

Radiation induced *in-situ* polymerization and crosslinking, which can be carried out at room temperature without initiators and catalysts, are safe, clean and effective method for synthesis of hydrogels [18–20], but radiation synthesis of organic/inorganic hybrid NC gels has not been reported, to the authors' knowledge.

A facile method for preparing NC gels using radiation technique has been developed. Neither initiator nor catalyst was used and the NC gels contained just PNIPAAm, clay and water. Hence, they are suitable for applications in biomedical fields. Effects of synthesis conditions on gel fraction, gel structure, mechanical strength, swelling behavior and thermo sensitivity of radiation synthesized NC gels (RNC gels) were studied. The formation mechanism of RNC gels was studied by microscopic Fourier transform infrared spectroscopy (Micro-FTIR), X-ray photoelectron spectroscopy (XPS), and thermogravimetric (TG) analyses.

II. EXPERIMENTAL

A. Materials

NIPAAm (97%, Aldrich Chemical Inc.) and synthetic hectorite "Laponite XLG" ($[Mg_{5.34}Li_{0.66}Si_8O_{20}(OH)_4]Na_{0.66}$, layer size Φ20–30 nm×1 nm, Rockwood Ltd.) were used as

* Supported by the National Natural Science Foundation of China (Nos. 91126014 and 11079007)
† Corresponding author, mlzhai@pku.edu.cn

received. Deionized water was used throughout the experiments.

B. Synthesis of RNC gels

The RNC gels were simply prepared by irradiating aqueous solutions consisting of monomers (NIPAAm) and clay. Laponite clay (0.61–5.47 g) and NIPAAm monomers (9.05 g) were dissolved in 40 mL of deionized water to form solutions, separately. Subsequently, they were mixed at 0 °C under stirring to form a uniform solution. The resulting solution was irradiated in air to 10 kGy, typically, with γ-rays in a ^{60}Co source (Peking University) to obtain RNC gels. The absorbed dose was measured with a Frick dosimetery system. Due to stabilizing effect of NIPAAm monomer on dispersion of laponite clay in water medium [12], the solution was very stable during the γ-irradiation process.

In order to investigate the cross-linking between laponite particles, the aqueous solutions of laponite clay (0.05 M and 0.09 M) were also irradiated to 10 kGy.

RNC gels with different clay contents were denoted as RNCn gels, in which "n" was defined as

$$n = 100c_{\rm l}/c_{\rm m}, \tag{1}$$

where $c_{\rm l}$ and $c_{\rm m}$ are molar concentrations of laponite clay and NIPAAm monomer in the solution, respectively. Clay contents of RNCn (n = 0, 1, 3, 5, 7, 9) gels are 0.00, 0.01, 0.03, 0.05, 0.07 and 0.09 M, respectively.

For SEM, Micro-FTIR, XPS, and TGA analyses, RNC gels were used after removal of sol part. For measurements of mechanical strength, as-prepared RNC gels were used directly in order to retain the original water/polymer ratio.

C. Mechanical strength of RNC gels

Compression measurements of RNC gels of Φ15 mm × 20 mm were performed at 25 °C in strain rate of 15% min^{-1} using an Instron-3365 material test system. The initial cross section was used to calculate the compression strength.

D. Gel fraction

The as-prepared RNC gels were cut into small pieces and vacuum-dried at 40 °C to constant weight. The dried RNC gels were immersed into deionized water at room temperature for 7 days to extract the sol part, and the deionized water was changed several times. RNC gels after removal of the sol part were vacuum-dried at 40 °C to constant weight. $G_{\rm f}$ was calculated using Eq. (2):

$$G_{\rm f} = (W_{\rm g}/W_0) \times 100\%, \tag{2}$$

where W_0 and $W_{\rm g}$ are weights of dried RNC gels before and after removal of the sol part, respectively.

E. Swelling behavior

Dried RNC gels were immersed in a large excess of deionized water at room temperature and taken out at desired time to be weighed. Excess water on gel surface was removed with filter paper before weighting. Eq. (3) was used to calculate the swelling ratio (*SR*)

$$SR = (W_t - W_0)/W_0, \tag{3}$$

where W_t is the weight of swollen gel at time t and W_0 is the weight of initial dried RNC gel.

Thermo sensitivity of the RNC gels was determined by observing their temperature-dependent equilibrium degree of swelling (*EDS*). Specifically, purified RNC gels were immersed in deionized water at a specific temperature for 84 h to reach swelling equilibrium. *EDS* of RNC gels was studied at 25–40 °C. *EDS* was calculated by Eq. (4)

$$EDS = (W_{\rm e} - W_0)/W_0, \tag{4}$$

where $W_{\rm e}$ is the weight of RNC gel in equilibrium state of swelling and W_0 is the weight of initial dried RNC gel.

F. Morphology of RNC gels

Morphology of the RNC gels was observed using SEM. In order to preserve the network structure, the RNC gels in equilibrium swollen state were immersed into liquid nitrogen and then lyophilized at −20 °C. The lyophilized RNC gels were coated with gold using an ion coater prior to photographing cross-sectional morphology. SEM images of the RNC gels were obtained using a Hitachi S-4800 instrument (Hitachi, Japanese) in high vacuum mode at 8.0 kV.

G. FTIR analysis

Micro-FTIR spectra of the samples were recorded using a Nicolet (NICOLETIN 10MX) spectrometer in absorbance mode in the range of 4000~600 cm^{-1}.

H. XPS analysis

XPS data of the RNC gels after removal of the sol part were obtained with an AXIS Ultra instrument from Kratos Analytical with low energy electron flooding for charge compensation. Monochromatic Al K_α ray was used. The data were converted into VAMAS file format, and Casa XPS software package was used for manipulation and curve-fitting.

I. TG analysis

TG analysis was carried out using a Q600 SDT instrument (TA Instruments, USA), at 25–700 °C in a heating rate of 10 °C/min under air atmosphere.

III. RESULTS AND DISCUSSION

A. Characterization of RNC gels

1. *Mechanical strength*

RNC gels containing a certain amount of clay have good optical transparency, high strength and flexibility (Fig. 1(a)). The as-prepared RNC3 gel can endure a large extent of deformation, while RNC0 gel is fragile and easily ruptures with slight stretch. The data in Table 1 indicate that the compression stress of an RNC gel at a certain strain increases with clay content. Specifically, RNC0 gel cannot endure compression deformation more than 90% and is crushed during the compression test, while, RNC3 gel does not show obvious rupture even under a compression strain of 95%, and it just returns to its initial shape when the compression test ends (Figs. 1(b)–1(d)). Apparently, mobility of the macromolecular chains in the network gives RNC3 gel high elasticity [12], and strong interaction between the clay sheets and the polymer matrix endows it with high mechanical strength. RNC5, RNC7, and RNC9 gels can also fully return to their initial shapes after compression to a strain of 95%, which is similar to the behavior displayed by RNC3 gel.

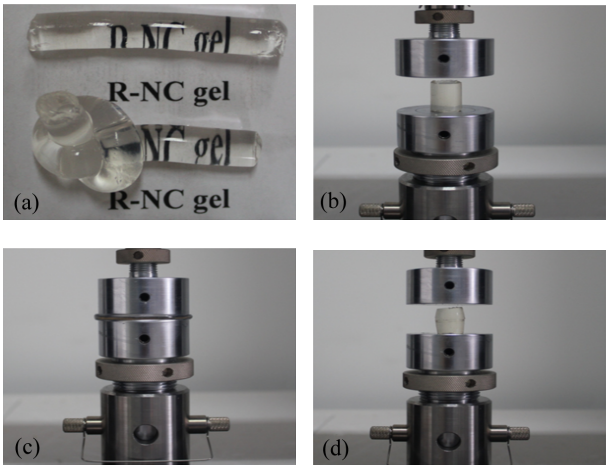

Fig. 1. (Color online) Photographs of RNC3 gel, (a) as prepared, (b) before compression, (c) at a compression strain of 95% and (d) after compression.

Figure 2 shows that compression stresses of the RNC gels increase slowly before 65% strain but rapidly under strains of 65–95%. The compression stresses of RNC3 gel are 0, 0.072 and 5.15 MPa at strains of 0%, 65% and 95%, respectively. The elastic modulus of an RNC gel is very low before 65% strain due to long flexible chains between crosslinking points. With the increase of strain, polymer chains gradually come close to their full extension, which causes higher elastic modulus and thus leads to a rapid increase of compression stress [21]. The compression stresses of RNC gels are comparable with those of NC gels prepared using other methods [14].

TABLE 1. Compositions, gel fractions, *EDS* and compression stresses of RNC gels synthesized at 10 kGy

RNC gel	Clay content (M)	G_f (%)	EDS_0 [a]	EDS_t [a]	$Stress_l$ [b] (MPa)	$Stress_h$ [b] (MPa)
RNC0	0	93.8	38.4	1.2	0.06	0.35
RNC1	0.01	94.2	29.0	1.4	0.28	1.21
RNC3	0.03	92.6	21.5	1.5	0.44	5.15
RNC5	0.05	93.3	18.7	1.8	0.66	9.68
RNC7	0.07	95.1	16.5	2.1	1.01	15.15
RNC9	0.09	96.0	14.1	2.6	1.53	19.43

[a] *EDS* at room temperature and 40 °C, respectively;
[b] Compression stress at low (80%) and high (95%) strain, respectively; Monomer contents of RNC gels are all 1.0 M.

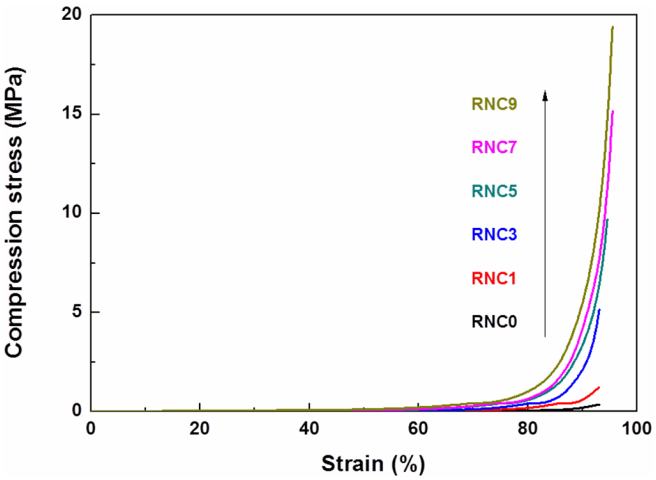

Fig. 2. (Color online) Stress-strain curves of RNC gels synthesized at 10 kGy.

2. *Gel fraction*

Absorbed dose affects gel formation of RNC gels in an analogous way, and the relationship between gel fraction and absorbed dose of RNC3 gel is illustrated in Fig. 3. The G_f increases sharply with the dose firstly and levels off at 5 kGy. Apart from RNC3 gel, gel fractions of other RNC gels are all above 90% at 10 kGy (Table 1). As a result, 10 kGy is suitable for preparing RNC gels with high performance. In addition, the solution containing mere laponite clay did not form gel after γ-irradiation. This indicates that irradiation cannot cause cross-linking between laponite particles.

3. *Swelling behavior*

As shown in Fig. 4, SR of RNC gel grows rapidly in the first 40 h, followed by slow increases towards its level off after 72 h. In Table 1, the *EDS* of RNC gel at room temperature decreases with increasing clay content. This indicates that crosslinking density increases when RNC gels incorporate more clay sheets in the polymer matrix. Shorter polymer chains between crosslinking points induce smaller pore size

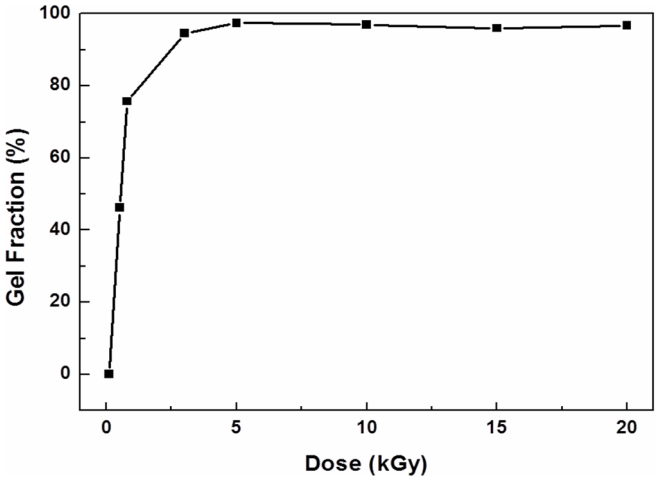

Fig. 3. Effect of absorbed dose on G_f of RNC3 gel.

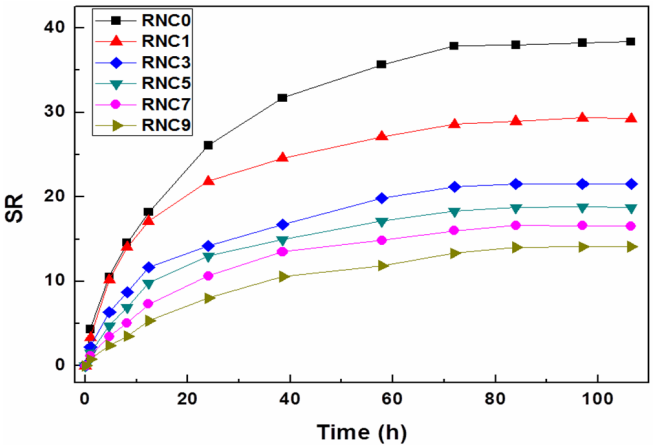

Fig. 4. (Color online) *SR* curves of RNC gels synthesized at 10 kGy.

TABLE 2. Data of swelling kinetics of RNC gels synthesized at 10 kGy

Parameters	RNC0	RNC1	RNC3	RNC5	RNC7	RNC9
$k_S \times 10^{-3}$ (h^{-1})	1.55	2.78	2.59	2.37	2.16	1.65
$S_{\infty,c}$ [a]	44.2	32.5	25.0	22.1	20.6	18.9
$S_{\infty,e}$ [a]	38.4	29.2	21.5	18.7	16.5	14.1
R_6 [b]	0.9979	0.9997	0.9984	0.9992	0.9985	0.9979

[a] Calculated and measured maximum swelling degrees, respectively;
[b] Correlation coefficient of Eq. (6).

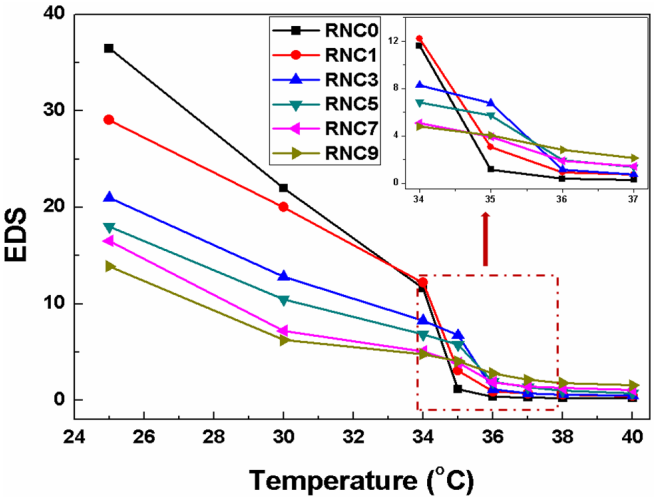

Fig. 5. (Color online) Temperature dependent *EDS* of RNC gels synthesized at 10 kGy.

in network of RNC gel and result in the decreased water absorption of RNC gel [22].

Scott proposed the following kinetics model to describe the swelling procedure of hydrogels [23]

$$\mathrm{d}S/\mathrm{d}t = k_S(S_\infty - S)^2. \quad (5)$$

With initial condition of $t = 0$ and $S = 0$, it can be deduced as Eq. (6)

$$t/S = A + Bt, \quad (6)$$

where k_S is the rate constant of swelling, S_∞ is the theoretical maximum swelling degree, $A = 1/k_S S_\infty^2 = 1(\mathrm{d}S/\mathrm{d}t)_0$, which is the reciprocal of initial swelling rate (r_0), and B is the reciprocal of S_∞. S_∞ and k_S can be calculated from the curve of $t/S \sim t$. The results are given in Table 2. The S_∞ values calculated by Eq. (6) ($S_{\infty,c}$) are close to those obtained from experiments ($S_{\infty,e}$), showing that the model fits the swelling behaviors of RNC gels, which is testified by the correlation coefficients. Generally, RNC gel with higher clay content possesses lower *EDS* and smaller rate constant, indicating that swelling behavior of RNC gel can be easily controlled by adjusting clay content.

The *EDS* of RNC gels (Fig. 5 and Table 1) decreases with increasing temperature, because at higher temperatures, hydrogen bonds between polymer chains and water molecules become weaker and the RNC gels become more and more hydrophobic interiorly. This is disadvantageous for polymer chains to bind water molecules and show higher water absorption. There is an abrupt decrease in *EDS* at 34 °C for RNC0 and RNC1 and at 35 °C for RNC3 and RNC5, while RNC7 and RNC9 do not show any sharp decrease in *EDS*.

Also, the *EDS* decreases gradually with the increasing clay content in RNC gels. This is because high clay content results in shorter polymer chains between crosslinking points and makes it difficult for polymer chains to aggregate together and show abrupt phase transition behavior in the macro level [15]. As a result, RNC gels lose their thermo sensitivity as clay content increases. Instead, they just show gradually decreased *EDS* with increasing temperature. *EDS* of RNCn gel at 40 °C is given in Table 1. RNC gel with higher clay content shows higher *EDS* at 40 °C due to its lower deswelling ratio.

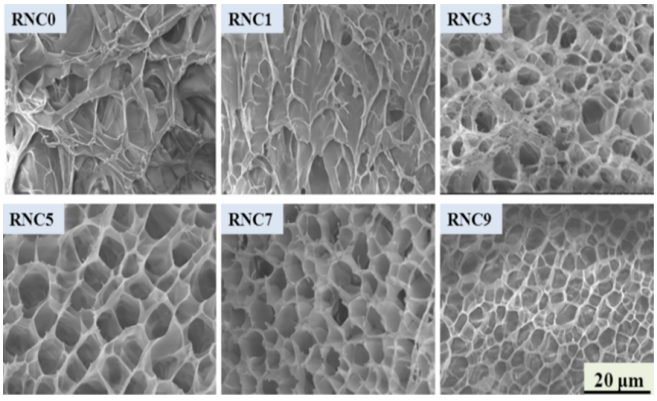

Fig. 6. (Color online) SEM images of RNC gels synthesized at 10 kGy.

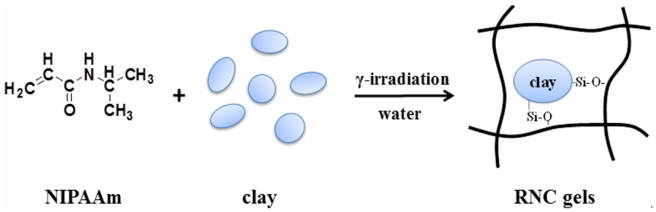

Fig. 7. (Color online) Formation mechanism of RNC gels under ionizing radiation.

4. *SEM images*

SEM images of lyophilized RNC gels are shown in Fig. 6. It can be found that homogenous three-dimensional network is formed in RNC gels. All the RNC gels are of cellular structures as normal hydrogels. The pore diameter decreases from dozens of micrometers to several micrometers with increasing clay content in swollen RNC gels. For example, the pore diameters are 15 in RNC0 and 7 μm in RNC9 gel. This is because RNC gel containing more clay sheets has higher crosslinking density, hence smaller pore size.

B. Formation mechanism of RNC gels

When the solution containing NIPAAm and clay is subjected to ionizing radiation, ·OH and ·H are formed. The two radicals can initiate polymerization and crosslinking of NIPAAm monomer. Also, they can react with Si−OH groups on surface of clay sheets to form Si−O· radicals, which can react with alkyl radicals of NIPAAm monomer or PNIPAAm polymer matrix, leading to the formation of chemical bonds between clay sheets and polymer matrix. In the prepared RNC gels, clay sheets act as crosslinkers to some extent.

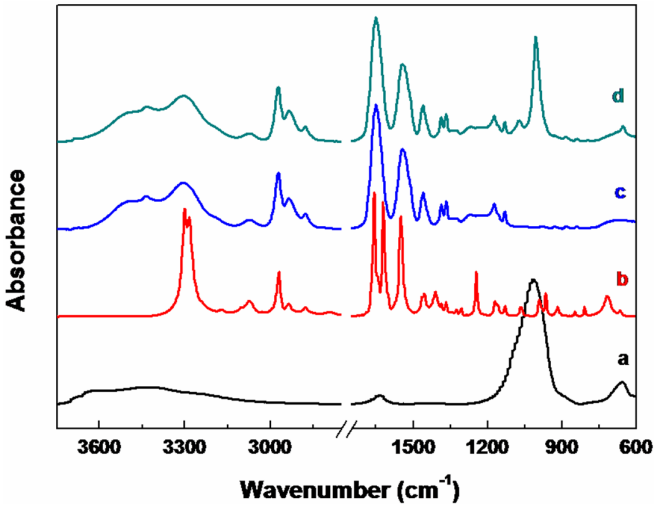

Fig. 8. (Color online) Micro-FTIR spectra of clay (a), NIPAAm (b), RNC0 gel (c) and RNC3 gel (d) synthesized at 10 kGy.

1. *FTIR analysis*

Micro-FTIR studies give information about components of RNC gels. FTIR spectrum of dried RNC3 gel (Fig. 8) shows both characteristic absorptions of PNIPAAm and clay. The absorption at 2 968 cm^{-1} is characteristic absorption of C−H bonds on saturated carbon atoms of PNIPAAm chains, while the absorption at 3 280 cm^{-1} is stretching vibration absorption of N−H bonds. The absorptions at 1665 and 1554 cm^{-1} are attributed to C=O bonds and C−N bonds, respectively. The absorptions at 1010 and 650 cm^{-1} are characteristic absorptions of clay and are attributed to Si−O bonds and Si−O−Si bonds, respectively [24]. Appearance of these absorptions indicates the incorporation of clay in RNC3 gel. The peaks at 1 616 cm^{-1} which is attributed to C=C bonds in NIPAAm monomers disappears in spectra of RNC0 gel and RNC3 gel. This indicates the occurring of polymerization and crosslinking of NIPAAm monomers.

In addition, no change in FTIR spectrum of RNC3 gel was observed even after its immersion in deionized water for up to three months (the deionized water was renewed regularly). This implies that there is hardly loss of clay from RNC3 gel in three months of soaking. Theoretically, if clay sheets are combined with polymer chains through physical interactions, the three months soaking may remove some clay sheets from the network structure of RNC3 gel. This implies some stronger interactions between clay sheets and polymer matrix, such as chemical interactions.

2. *XPS analysis*

The XPS spectra (Fig. 9) provide more proof of chemical interactions between polymer chains and clay sheets. An obvious peak of Mg appears in spectrum of RNC3 gel due to incorporation of clay. The C 1s XPS spectrum of RNC0 gel shown in Fig. 9(b) exhibits three peaks centered at 284.8,

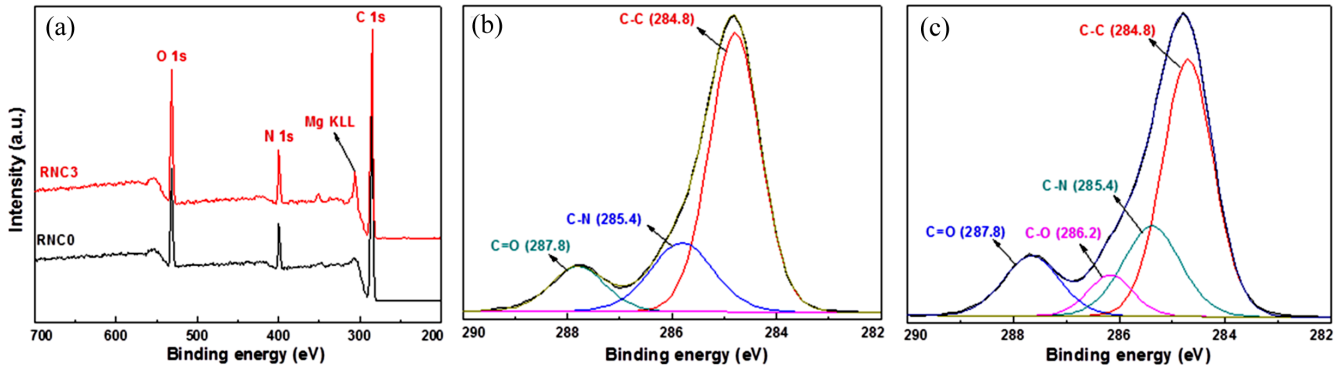

Fig. 9. (Color online) Low resolution XPS spectra of RNC gels (a), C 1s XPS spectrum of RNC0 gel (b) and C 1s XPS spectrum of RNC3 gel (c).

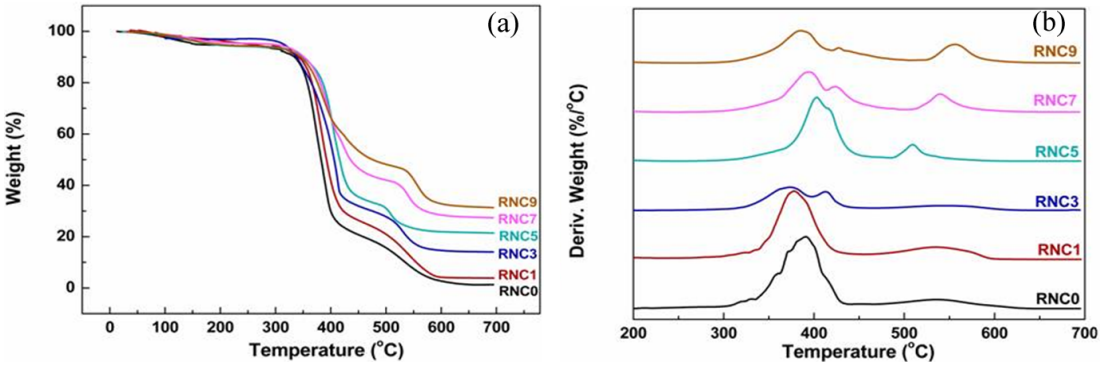

Fig. 10. (Color online) TG (a) and DTG (b) curves of RNC gels synthesized at 10 kGy.

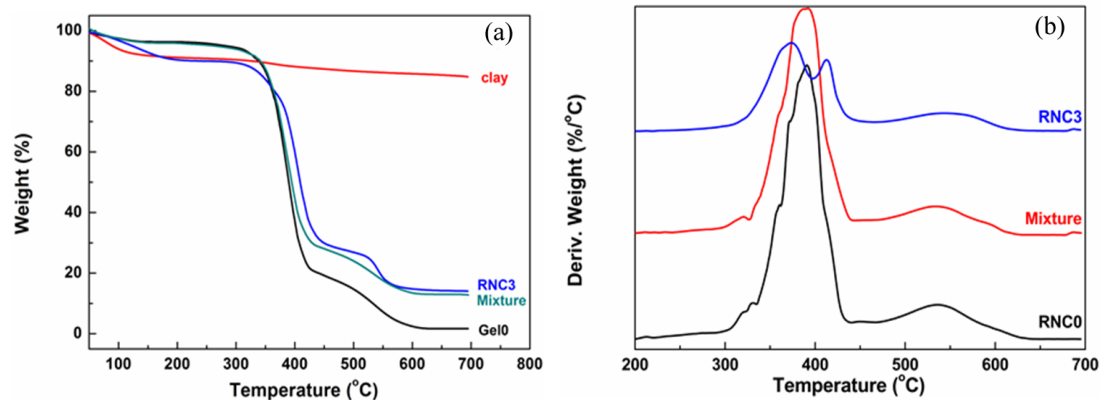

Fig. 11. (Color online) TG (a) and DTG (b) curves of 10 kGy-irradiated clay, RNC3 gel, physical mixture sample and RNC0 gel.

285.4 and 287.8 eV, which are assigned to C−C bonds, C−N bonds and C=O bonds, respectively [25].

In C 1s XPS spectrum of RNC3 gel (Fig. 9(c)), the new peak centered at 286.2 eV is attributed to C−O bonds, which should be resulted from chemical bonds between polymer chains and clay sheets. Considering reactions that may occur under irradiation, the C−O single bond can be formed from carbon atoms of alkyl radicals and oxygen atoms of Si−O·.

3. *TG analysis*

TG and DTG curves of RNC gels are shown in Figs. 10 and 11. The PNIPAAm portion in RNC gels almost decomposes completely at 700 °C under air atmosphere and the final weight represents clay contents in RNC gels. The TG analysis results are listed in Table 3. It is found that experimental residual of RNC gels containing clay is slightly less than the-

TABLE 3. Data of TG analysis of RNC gels synthesized at 10 kGy

RNC gel	T_d2[a] (°C)	WR_a[b] (%)	$WL2$[c] (%)	T_d3[a] (°C)	WR_b[b] (%)	$WL3$[c] (%)	Rsd_t[d] (%)	Rsd_e[d] (%)
RNC0	308.6	76.9	77.0	426.0	23.1	21.1	0	0
RNC1	310.4	72.0	69.03	435.8	21.7	21.1	6.3	5.28
RNC3	309.4	58.2	58.5	479.4	20.2	19.5	16.8	14.6
RNC5	310.5	57.5	57.1	492.3	17.3	16.6	25.2	23.4
RNC7	311.8	52.2	54.6	501.6	15.7	15.9	32.1	29.4
RNC9	309.9	47.9	48.3	516.9	14.4	14.7	37.8	34.4

[a] The onset temperature of decomposition of the 2nd and 3rd degradation of RNC gels, respectively.
[b] Weight ratio of acylamino groups and −C−C− backbones in RNC gels, respectively.
[c] Wight loss of the 2nd and 3rd degradation, respectively.
[d] Theoretical and experimental residual weight of RNC gels, respectively.

oretical residual. This may result from weight loss of clay portion in RNC gels. In Fig. 11(a), pure clay sample shows a weight loss of 14.7% when heated to 700 °C. Weight loss of clay might be caused by loss of bounded water in clay, or conversion of alkali to metallic oxide.

TG and DTG curves in Fig. 10 show that RNC gels experience three steps of degradation. According to Ref. [26], the first degradation starting at about 50 °C is the loss of residual water in structures of RNC gels. The second one is attributed to decomposition of acylamino groups in RNC gels, because the data in Table 3 imply that weight ratios of acylamino groups in RNC gels are quite close to the weight loss ratios of the second degradations. The third degradation is attributed to breakage of −C−C− backbones in RNC gels and the data in Table 3 support this deduction.

From DTG curves in Fig. 10(b) and Table 3, the onset temperature of decomposition of both the second and third degradation increases with the content of clay sheets, and the order is: RNC0≤RNC1<RNC5<RNC7<RNC9. These indicate that the formation of chemical bonds between polymer chains (including acylamino groups and −C−C− backbones) and clay sheets. It is also found that only one peak arises in the process of the second degradation of RNC0 and RNC1 gel, while there are two for RNC3, RNC5, RNC7 and RNC9 gels. The emerging peak in the process of the second degradation further indicates that there are chemical interactions between acylamino groups and clay sheets. However, effect of chemical interactions between acylamino groups and clay sheets in RNC0 and RNC1 gels is not strong enough to cause this change due to low contents of clay.

In addition, TG curves of physical mixture of RNC0 gel and radiated clay, RNC0 gel, radiated clay and RNC3 gel are shown together in Fig. 11. It is obvious that TG and DTG curves of RNC0 gel and the physical mixture sample are quite similar, while they are different from those of RNC3 gel. The third degradation of RNC3 gel starts at a higher temperature than those of RNC0 gel and the physical mixture sample. As hydrogen bonds or other physical forces are not effective in such a high temperature [27], some stronger interactions must exist between polymer chains and clay sheets in the network of RNC gels. It can be concluded that chemical bonds (like C−O bonds) between polymer matrix and clay sheets are formed during radiation process from XPS, TG and DTG analyses.

IV. CONCLUSION

NC gels based on PNIPAAm/clay system were successfully synthesized by radiation method for the first time. The novel RNC gel has good optical transparency, high strength, regular swelling behavior and thermo sensitivity. Micro-FTIR, XPS and TG analyses proved that chemical bonds between polymer matrix and clay sheets were formed during γ-irradiation. This work presents a new method for preparing high performance hydrogels, and these RNC gels are more suitable for applications in biomedical field due to the absence of residual initiators and catalysts.

[1] Jiang Y M, Li B, Chen X J, *et al*. J Appl Polym Sci, 2012, **125**: E148–E156.
[2] Li Y Y and Fan X D. Polymer, 2002, **43**: 4997–5003.
[3] Zhu C H, Lu Y, Peng J, *et al*. Adv Funct Mater, 2012, **22**: 4017–4022.
[4] Wu J J, Ren Y, Sun J Z, *et al*. ACS Appl Mater Interfaces, 2013, **5**: 3519–3523.
[5] Li X, Austin B, Isner J, *et al*. J Appl Polym Sci, 2013, **128**, 1804–1814.
[6] He X L, Yu S, Dong Y Y, *et al*. J Mater Sci, 2009, **44**: 4078–4086.
[7] Lee D S, Choi H J, Chuang K H, *et al*. Sensor Actuat B-Chem, 2008, **130**: 150–157.
[8] Liu M Q, Liu H Y, Bai L G, *et al*. J Mater Sci, 2011, **46**: 4820–4825.
[9] Petrusic S, Jovancic P, Lewandowski M, *et al*. J Mater Sci, 2013, **48**: 7935–7948.
[10] Okumura Y and Ito K. Adv Mater, 2001, **13**: 485–487.
[11] Muñoz-Muñoz F, Bucio E, Magariños B, *et al*. J Appl Polym Sci, 2014, **131**: 39992.
[12] Haraguchi K and Takehisa T. Adv Mater, 2012, **14**: 1120–1124.

[13] Haraguchi K and Li H J. Macromolecules, 2006, **39**: 1898–1905.
[14] Rohan L, Elizabeth A L, Saleh A J. J Appl Polym Sci, 2012, **125**: 369–381.
[15] Haraguchi K and Takada T. Macromolecules, 2010, **43**: 4294–4299.
[16] Daniel L M, Frost R L, Zhu H Y. J Colloid Interf Sci, 2008, **321**: 302–309.
[17] Haraguchi K, Uyama K, Tanimoto H. Macromol Rapid Comm, 2011, **32**: 1253–1258.
[18] Li C C, Zhai M L, Peng J, *et al*. Polymer, 2009, **50**: 4888–4894.
[19] Killion J A, Geever L M, Devine D M, *et al*. J Mater Sci, 2012, **47**: 6577–6585.
[20] Abd El-Rehim H A, Hegazy E A, Hamed A A, *et al*. Eur Polym J, 2013, **49**: 601–612.
[21] Haraguchi K, Farnworth R, Ohbayashi A, *et al*. Macromolecules, 2003, **36**: 5732–5741.
[22] Huang T, Xu H G, Jiao K X, *et al*. Adv Mater, 2007, **19**: 1622–1626.
[23] Scott H J. J Macromol Sci B, 1992, **31B**: 1–9.
[24] Haraguchi K, Xu Y J, Li G. Macromol Rapid Comm, 2010, **31**: 718–723.
[25] Moulder J F, Stickle W F, Sobol P E, *et al*. Handbook of X-ray Photoelectron Spectroscopy, Perkin-Elmer Corporation (Physical electronics), Minnesota, 1992.
[26] Ricardo G S, Welington F M, Roberto F S F. Polym Degrad Stabil, 1998, **61**: 275–281.
[27] Qiu J Y, Xu L, Peng J, *et al*. Carbohyd Polym, 2007, **70**: 236–242.